Electronic Supplementary Material (ESI) for Physical Chemistry Chemical Physics.

Tunable electronic properties of BSe-MoS_2/WS_2 heterostructures for a promoted light utilization

Honglin Li, Lijuan Ye, Yuanqiang Xiong, Hong Zhang, Shuren Zhou, Wanjun Li**

College of Physics and Electronic Engineering, Chongqing Normal University, Chongqing 401331, PR China

**E-mail: liwj@cqnu.edu.cn (Wanjun Li), xyq.0810@163.com (Yuanqiang Xiong)*

COMPUTATIONAL METHODS

In this work, the initial models of different structures were built using VESTA. [1] First-principles calculations are performed by using the density functional theory (DFT) approach with the projector-augmented-wave (PAW) method. [2-6] For the exchange and correlation energies, the generalized gradient approximation (GGA) in the form of Perdew–Burke–Ernzerhof (PBE) functional is adopted.[7] Considering the reality that the vdW interaction has an unneglected effect on the final stability of the heterostructures, the standard PBE function cannot handle this weak interaction well, so we adopted the DFT-D2 method advanced by Grimme to describe the weak vdW interaction between the two monolayers in all calculations, [8] in which all the force field parameters are obtained based on the PBE function. The total energy (E_{total}) is expressed as: $E_{total} = E_{KS}\text{-}DFT + E_{vdW}$, where $E_{KS}\text{-}DFT$ and E_{vdW} are Kohn-Sham DFT energy and dispersion correction respectively. [9, 10] The first Brillouin-zone sampling of 5×5×1 and 11×11×1 k-points generated by Monkhorst-Pack scheme are used for geometric optimization and optical property calculations, respectively. The vacuum layer is set to 20 Å along *Z* direction to avoid the interactions induced by the periodic effects. To find a balance between accuracy and efficiency, a 500 eV cut-off energy has been adopted in all calculations. We have performed convergence test calculations using more strict calculation parameters, a stricter cutoff energy (up to 600 eV) and k-point sampling (up to 7×7×1) as shown in Figure S1 and S2. We found that the main results are not influenced by the strict parameters, compared with k-point sampling 5×5×1 and cutoff energy convergence criterion of 500 eV. The

pristine and heterostructures were optimized until the forces on each atom are less than 10^{-4} eV and the Hellmann–Feynman force on each atom is 0.01 eV $Å^{-1}$, which was sufficient precise to reach convergence for the whole calculations. It should be pointed out that Mo-based and W-based materials show the strong spin-orbital couplings (SOC), [11, 12] so SOC is included in all calculations. In order to study the optical absorption property of BSe and XS_2 monolayers as well as vdW heterostructures, the dielectric constants need to be obtained. The frequency dependent complex dielectric function is formed by adding the real and imaginary parts as: $\varepsilon(\omega)= \varepsilon_1(\omega)+i\varepsilon_2(\omega)$. The imaginary part $\varepsilon_2(\omega)$ can be obtained by summing up enough empty band states by the following formula, [13]

$$\varepsilon_2(\omega) = \frac{4\pi^2 e^2}{\Omega}\lim_{q\to 0}\frac{1}{q^2}\sum_{c:v:k} 2\omega_k \delta(\in_{ck} - \in_{vk} - \omega) \times \left\langle u_{ck+e_\alpha q}|u_{vk}\right\rangle \left\langle u_{ck+e_\beta q}|u_{vk}\right\rangle^* \quad (1)$$

where Ω stands for the volume, α and β are the Cartesian components, e_α and e_β are the unit vectors, *v* and *c* represent matrix elements of the transition from the valence band state (u_{vk}) to the conduction band state (u_{ck}), $\in_{ck}$ and $\in_{vk}$ denote for the energy of the conduction and valence band respectively. The real part $\varepsilon_1(\omega)$ is derived from the Kramers–Kronig equation, [14]

$$\varepsilon_1(\omega) = 1 + \frac{2}{\pi}P\int_0^\infty \frac{\varepsilon_2^{\alpha\beta}(\omega')\omega'}{\omega'^2 - \omega^2 + i\eta}d\omega' \quad (2)$$

where P represents the principal value of the integral. From these two parts of the dielectric functions, the absorption coefficient $\alpha(\omega)$ can be obtained by using the following formula. [15]

$$\alpha(\omega) = \sqrt{2}\,\omega\{[\varepsilon_1^2(\omega) + \varepsilon_2^2(\omega)]^{\frac{1}{2}} - \varepsilon_1(\omega)\}^{\frac{1}{2}} \quad (3)$$

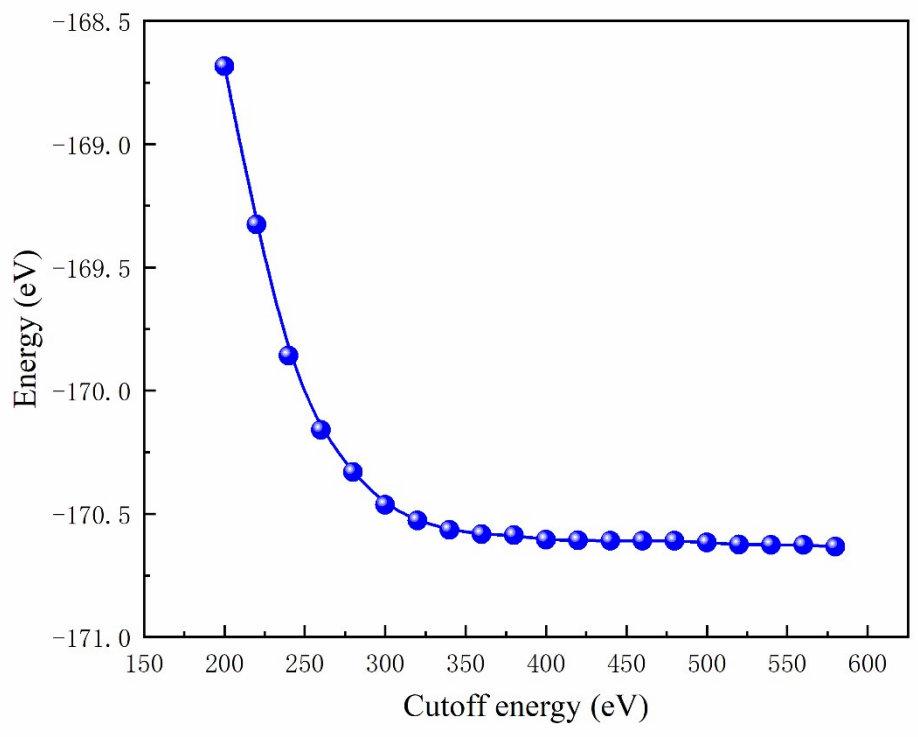

Figure S1. Cutoff energy convergence test of BSe-MoS_2 heterostructure.

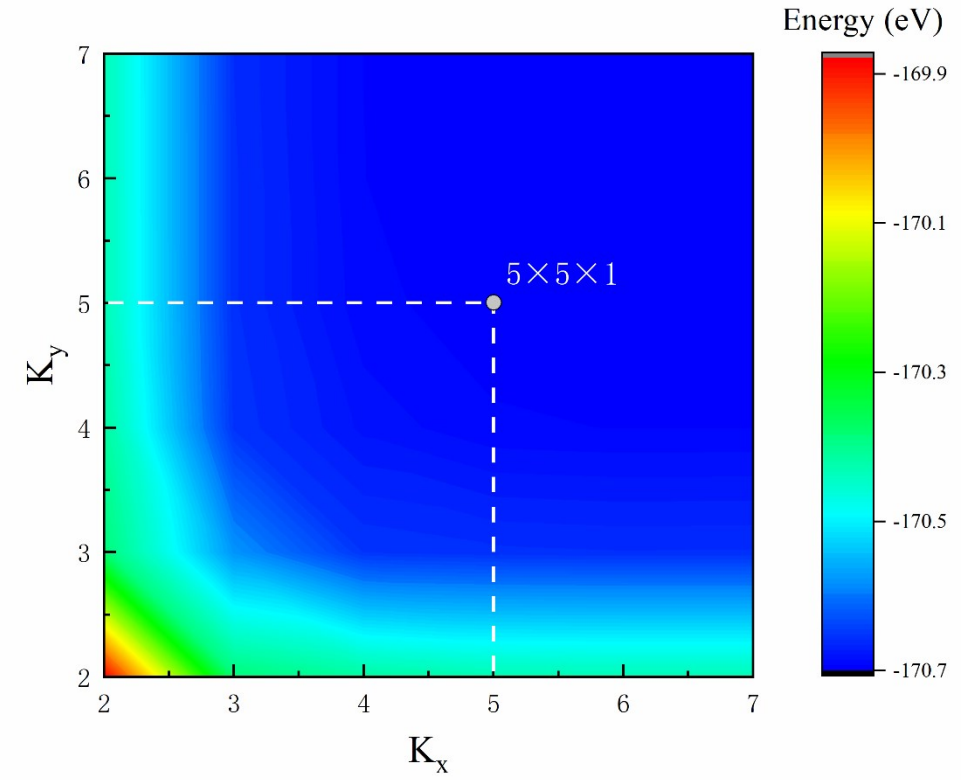

Figure S2. KPOINTS convergence test of BSe-MoS_2 heterostructure.

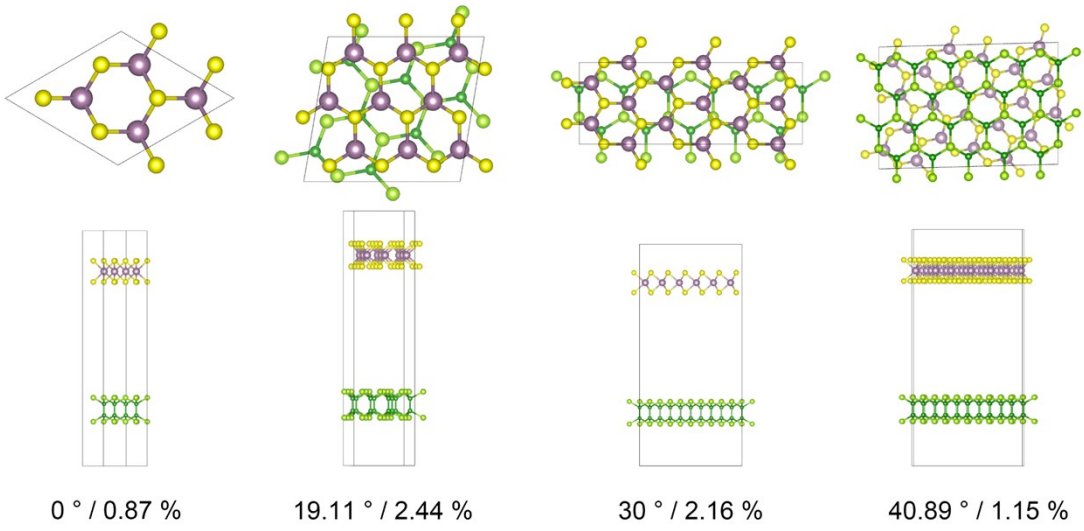

Figure S3. Four twisted BSe-MoS_2 heterostructures before spacing optimization.

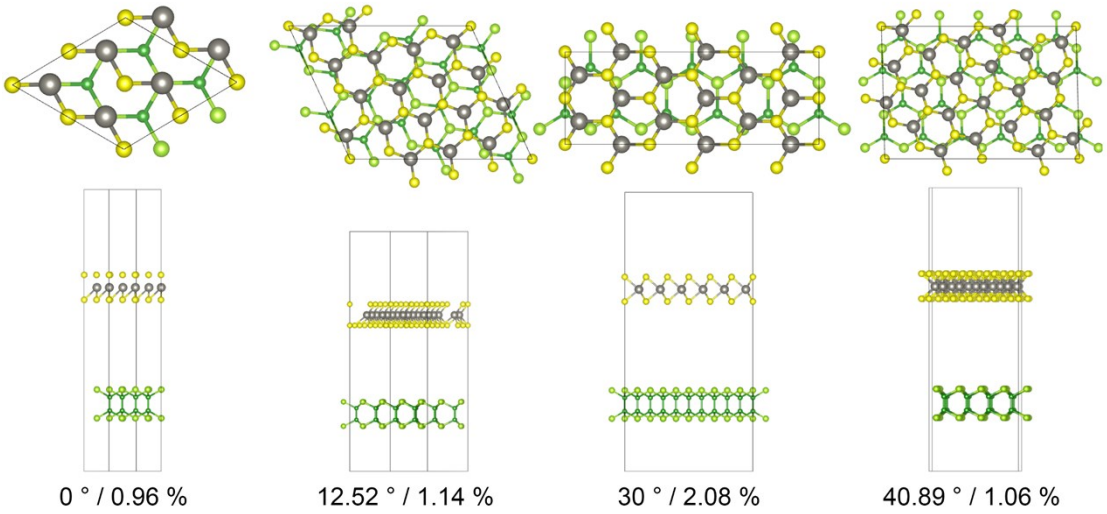

Figure S4. Four twisted BSe-WS_2 heterostructures before spacing optimization.

Table S1. The lattice constants of BSe-XS_2 heterostructures under three strained (**S-**) approaches before spacing optimization.

/	**BSe-MoS_2**			**BSe-WS_2**		
	S-BSe	**S-MoS_2**	**S-equally**	**S-BSe**	**S-WS_2**	**S-equally**
a/Å	3.16	3.25	3.21	3.16	3.25	3.20
b/Å	3.16	3.25	3.27	3.16	3.25	3.27
c/Å	35.34	35.34	35.34	35.42	35.42	35.42
α*/degree*	90	90	90	90	90	90
β*/degree*	90	90	90	90	90	90
γ*/degree*	60	60	60.65	60	60	60.71
V/*Å³*	306.77	323.27	323.21	305.92	324.00	323.93

REFERENCES

1. Momma, K.; Izumi, F., VESTA 3 for three-dimensional visualization of crystal, volumetric and morphology data. *Journal of applied crystallography* **2011,** *44* (6), 1272-1276.
2. Pan, J.; Shao, X.; Xu, X.; Zhong, J.; Hu, J.; Ma, L., Organic Dye Molecules Sensitization-Enhanced Photocatalytic Water-Splitting Activity of MoS_2 from First-Principles Calculations. *The Journal of Physical Chemistry C* **2020,** *124* (12), 6580-6587.
3. Zhang, W.; Zou, G.; Choi, J.-H., Adsorption Behavior of the Hydroxyl Radical and Its Effects on Monolayer MoS_2. *ACS omega* **2020,** *5* (4), 1982-1986.
4. Li, J.; Zhang, S.; Wang, Y.; Duan, H. M.; Long, M., First-Principles Study of Strain Modulation in S_3P_2/Black Phosphorene vdW Heterostructured Nanosheets for Flexible Electronics. *ACS Applied Nano Materials* **2020,** *3* (5), 4407-4417.
5. Lee, J.; Huang, J.; Sumpter, B. G.; Yoon, M., Strain-engineered optoelectronic properties of 2D transition metal dichalcogenide lateral heterostructures. *2D Materials* **2017,** *4* (2), 021016.
6. Lou, P.; Lee, J. Y., GeC/GaN vdW Heterojunctions: A Promising Photocatalyst for Overall Water Splitting and Solar Energy Conversion. *ACS Applied Materials & Interfaces* **2020,** *12* (12), 14289-14297.
7. Zhou, Z.; Zhang, Y.; Zhang, X.; Niu, X.; Wu, G.; Wang, J., Suppressing photoexcited electron–hole recombination in $MoSe_2$/WSe_2 lateral heterostructures via interface-coupled state engineering: a time-domain ab initio study. *Journal of Materials Chemistry A* **2020,** *8* (39), 20621-20628.

8. Grimme, S., Semiempirical GGA-type density functional constructed with a long-range dispersion correction. *Journal of computational chemistry* **2006,** *27* (15), 1787-1799.

9. Han, S. W.; Kwon, H.; Kim, S. K.; Ryu, S.; Yun, W. S.; Kim, D. H.; Hwang, J. H.; Kang, J. S.; Baik, J.; Shin, H. J., Band-gap transition induced by interlayer van der Waals interaction in MoS_2. *Physical Review B* **2011,** *84* (4), 045409.

10. Ataca, C.; Sahin, H.; Ciraci, S., Stable, single-layer MX_2 transition-metal oxides and dichalcogenides in a honeycomb-like structure. *The Journal of Physical Chemistry C* **2012,** *116* (16), 8983-8999.

11. Wang, J.; Shu, H.; Zhao, T.; Liang, P.; Wang, N.; Cao, D.; Chen, X., Intriguing electronic and optical properties of two-dimensional Janus transition metal dichalcogenides. *Physical Chemistry Chemical Physics* **2018,** *20* (27), 18571-18578.

12. Rasmussen, F. A.; Thygesen, K. S., Computational 2D materials database: electronic structure of transition-metal dichalcogenides and oxides. *The Journal of Physical Chemistry C* **2015,** *119* (23), 13169-13183.

13. Li, Y.; Liu, J.; Zhao, X.; Yuan, X.; Hu, G.; Yuan, X.; Ren, J., Strain forces tuned the electronic and optical properties in GaTe/MoS_2 van der Waals heterostructures. *RSC Advances* **2020,** *10* (42), 25136-25142.

14. Eberlein, T.; Bangert, U.; Nair, R. R.; Jones, R.; Gass, M.; Bleloch, A. L.; Novoselov, K. S.; Geim, A.; Briddon, P. R., Plasmon spectroscopy of free-standing graphene films. *Physical Review B* **2008,** *77* (23), 233406.

15. Luo, B.; Wang, X.; Tian, E.; Li, G.; Li, L., Electronic structure, optical and dielectric properties of $BaTiO_3$/$CaTiO_3$/$SrTiO_3$ ferroelectric superlattices from first-principles

calculations. *Journal of Materials Chemistry C* **2015,** *3* (33), 8625-8633.